Understanding Precipitator Performance via CFD Modelling

Yuqing Feng [1], Lachlan Graham[2], Peter Witt[3], Bon Nguyen[4] and Yuanlong Huang[5]
1. Principal Research Scientist
2. Senior Research Engineer
3. Senior Principal Research Scientist
4. Senior Experimental Research Scientist
CSIRO Mineral Resources Research Unit - Processing Program, Clayton, Australia
5. Head of new type agitator division
Shenyang Aluminium and Magnesium Engineering & Research Institute (SAMI), Shenyang, China
Corresponding author: yuqing.Feng@csiro.au
https://doi.org/10.71659/icsoba2025-aa027

Abstract

CSIRO has a long-standing history of working with alumina refineries to investigate the hydrodynamics of precipitators. This includes the effects of draft tubes, multiple impeller systems, and SWIRLFLOW® impeller retrofits. While physical modelling has traditionally been the foundation of this research, the use of computational fluid dynamics (CFD) has always been a significant component of the work to support the optimisation of agitation systems that often goes unmentioned. Key areas of investigation include scale formation, particle suspension, heat transfer, and power consumption.

In this study, laboratory-scale analogue tanks were used to establish CFD calculated wall shear stress as a practical proxy for predicting scale formation. Measured scale thickness and total scale mass were compared with CFD-predicted wall shear stress. The results revealed that low-shear regions are related with heavy scale accumulation. The total scale mass was found to decrease with increasing shear stress, reinforcing the predictive capability of CFD.

The CFD model was extended to compare the hydrodynamic performance of industrial-scale draft tube and SWIRLFLOW® tanks. The analysis showed that the SWIRLFLOW® configuration generates a more uniform wall shear stress distribution and stronger upward flow, effectively reducing the potential for both scale formation and wall erosion. In contrast, the draft tube tank exhibited pronounced low-shear regions along the upper section of the tank wall and the outer surface of the draft tube – features consistent with severe scaling observed in practice and, in some cases, structural failure due to excessive scale buildup.

CFD also provided insights into the effect of agitation strategies on particle breakup in precipitators by comparing turbulent microscales for the draft tube and SWIRLFLOW® tanks.
These results confirm that CFD, when validated against experimental observations, provides a robust framework for understanding scale formation mechanisms and for optimising the design and operation of industrial precipitator tanks. CFD now plays a vital role in complementing physical experimentation, delivering insights into precipitator performance that are otherwise difficult or impractical to obtain through laboratory studies alone.

Keywords: Precipitation tank, Swirl flow, Scale, CFD, Draft tube.

1. Introduction

Scale formation continues to be a persistent and costly issue in stirred slurry tanks, particularly within hydrometallurgical, chemical, and mineral processing operations. It contributes to

increased maintenance, reduced equipment longevity, and impaired process efficiency. Over several decades, CSIRO has partnered with the alumina industry to improve the understanding and control of such issues in precipitation tanks [1]. These efforts have explored the effects of agitation systems—including draft tubes, multiple impeller arrangements, and SWIRLFLOW® retrofits—using both physical experiments and computational fluid dynamics (CFD).

To support scale control strategies, CSIRO developed a novel analogue scale formation system using a controlled gypsum precipitation reaction within geometrically scaled 2 litre and 50 litre laboratory tanks. These experiments allowed systematic evaluation of scale morphology and distribution under different agitation conditions, generating data that closely resembled patterns observed in full-scale industrial operations. Based on these insights, wall shear stress was identified as a potential and practical CFD-accessible proxy for predicting scale formation.

Some hydrodynamic parameters in alumina precipitators are difficult or impractical to measure at laboratory or plant scale, making CFD a valuable complementary tool. In this work, CFD models were benchmarked against experimental results and then extended to assess performance across different precipitator configurations. Key analyses undertaken included:

- A correlation between experimentally measured scale thickness and CFD-predicted wall shear stress in lab-scale tanks, validating the use of shear stress as a proxy for scale propensity,
- A comparative CFD study of industrial-scale draft tube and SWIRLFLOW® designs, evaluating their impact on scale mitigation and flow distribution.

CFD was also used to provide evaluation of turbulence microscales to determine whether there was a significant difference between draft tube and SWIRLFLOW® agitation in terms of agglomeration or particle breakage.

2. CFD Model

2.1 Model Description

CFD simulations were performed by solving the Reynolds-averaged Navier–Stokes (RANS) equations, which govern the conservation of mass and momentum for incompressible turbulent flows. During the early stages of model development, several turbulence models were evaluated, including the standard k–ε, Shear Stress Transport (SST), and Reynolds Stress Model (RSM), to determine the most suitable approach for representing the highly swirling and recirculating flows typical of precipitator tanks. The RSM was ultimately selected due to its ability to resolve the transport of individual Reynolds stress components, offering improved accuracy in capturing anisotropic turbulence and swirling motion near impellers. This advanced turbulence modelling approach enables a more detailed representation of flow structure, particularly in regions critical for scale formation and solids suspension.

Various methods are available to model rotating impellers in CFD simulations, including the transient sliding mesh approach and steady-state techniques such as the frozen rotor. The sliding mesh approach captures full transient interactions between rotating and stationary zones, while Frozen rotor methods assume steady-state conditions, modelling the impeller region in a rotating reference frame and apply averaging across the interface between the rotating and stationary tank domains. These steady-state approaches are computationally efficient and well suited for predicting mean flow structures in mixing tanks. In this study, steady-state simulations using the frozen rotor method were initially performed to obtain a converged flow field, which then served as the initial condition for transient simulations using the sliding mesh approach. The transient simulations captured unsteady flow behaviour, and time-averaged results were extracted for

comparison with experimental data and steady-state predictions. This hybrid strategy combined computational efficiency during model initialisation with improved accuracy in resolving unsteady flow structures critical to scale formation and solids suspension.

2.2 Geometry, Meshing and Boundary Conditions

Figure 1 shows schematic drawings of the SWIRLFLOW® and draft tube tank geometries. The SWIRLFLOW® tank is characterized by an open tank configuration with a centrally mounted radial impeller that generates a strong swirling motion. In contrast, the draft tube tank features a vertical draft tube housing an axial-flow impeller, promoting circulation through the tube and recirculation outside it.

For the laboratory-scale analogue tanks, two sizes were used: 2 litres and 50 litres. To compare the performance of SWIRLFLOW® and draft tube configurations, a representative industrial-scale geometry was adopted based on typical design proportions used in alumina refineries, although not specific to any single plant. The key geometric parameters and operating conditions used in the simulations are summarised in Table 1. Both laboratory-scale tanks were fitted with CSIRO's SWIRLFLOW® SF-C1 impellers of different diameters. In the industrial-scale simulations, the SWIRLFLOW® tank employed the SF-A impeller design, while the draft tube tank used an Airfoil C200 impeller positioned within the draft tube. Figure 2 presents 3D images of the different impeller designs used in this study.

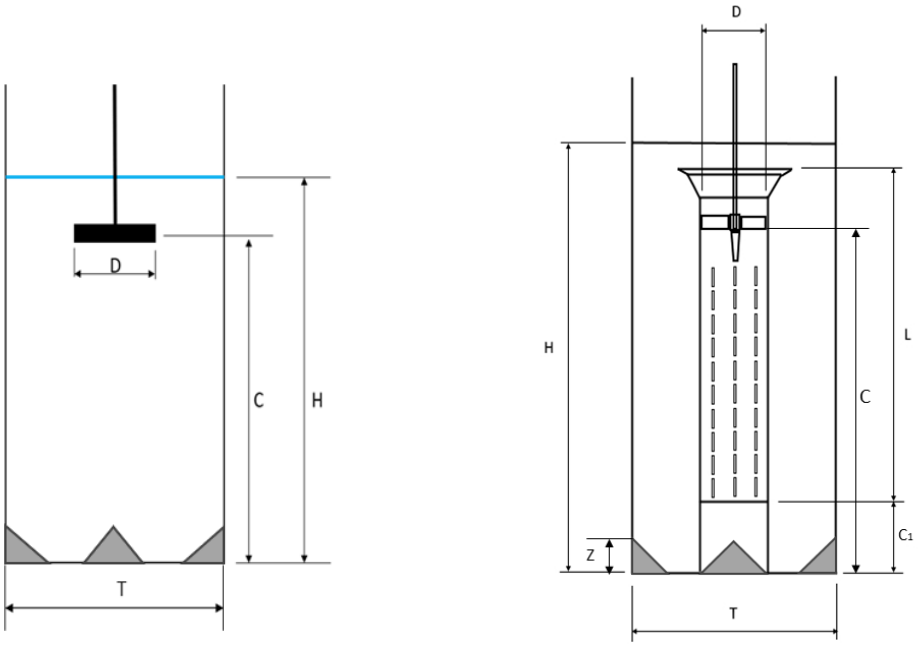

(a) (b)

Figure 1. Schematic representation of dimensional parameters for (a) a typical SWIRLFLOW® tank and (b) a draft tube tank.

Geometry and meshing were performed using Ansys DesignModeler and Ansys Meshing, respectively. Simulations were conducted in Ansys CFX (Release 23.1), and results were post-processed using CFD-Post. The CFD geometries for the two lab-scale tanks (2 L and 50 L) are shown in Figure 3, while those for the full-scale precipitation tanks are presented in Figure 4. Computational domain was divided into two regions: a cylindrical rotating zone enclosing the impeller and a stationary zone for the remainder of the tank. Unstructured meshes were generated for both zones, with local refinement near the impeller to accurately capture velocity and shear

gradients. The top free surface was simplified as a free-slip flat wall to reduce computational complexity. Figure 5 provides a close-up view of the mesh in the impeller region, highlighting the use of an inflation layers on the impeller blades to resolve near-wall flow behaviour.
As described in the previous section, the Multiple Reference Frame Frozen Rotor approach was first used to obtain a steady-state solution, which was then employed as the initial condition for a sliding mesh transient simulation. Strong swirling motion in the tank can cause a concave deformation at the liquid surface, this effect was neglected in the model by treating the top surface as flat and free-slip.

Table 1: Geometrical parameters and operating conditions of different tanks.

Tank Name	2 L Lab Tank	50 L Lab Tank	Industrial SF Tank	Industrial Draft Tube Tank
Impeller type	SF-C1	SF-C1	Sf-A	Airfoil C200
Tank diameter (T), (m)	0.122	0.396	13.4	13.8
Impeller diameter (D), (m)	0.05	0.11	4.29	3.73
Liquid height (H), (m)	0.125	0.4	32.9	32.17
Clearance (C), (m)	0.04	0.25	30.4	25.973
Rotation speed (rpm)	150-500	150-300	16.32	37.8
Liquor density (kg/m^3)	1000	1000	1270	1270
Slurry density (kg/m^3)			1413	1413
Liquor viscosity (Pa s)	0.0009	0.0009	0.0017	0.0017
Solid density (kg/m^3)			2422	2422
Solid volume fraction (-)			0.12	0.12
Solid mass fraction (-)			0.21	0.21
Draft tube diameter, (m)				4.14
Draft tube length (L), (m)				24.6
Draft tube clearance height (C_1), (m)				4.14
Fillet height (Z), (m)				2.12

(a) **(b)** **(c)**

Figure 2. 3D images showing the structure of different impellers: (a) SWIRLFLOW® SF-C1; (b) SWIRLFLOW® SF-A; (c) draft tube Airfoil C200 impeller.

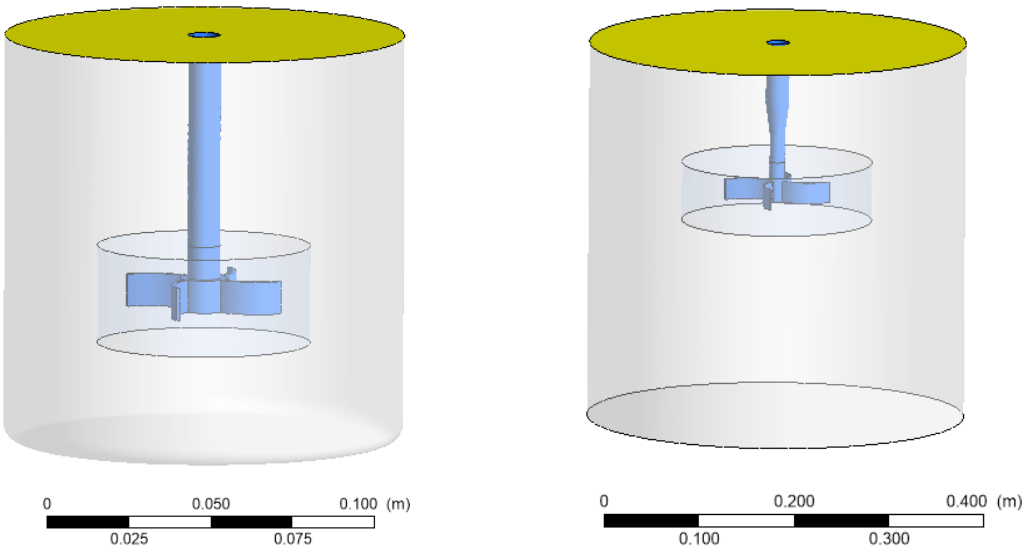

(a) (b)

Figure 3. Geometries generated using Ansys DesignModeler: (a) 2 L tank; (b) 50 L tank.

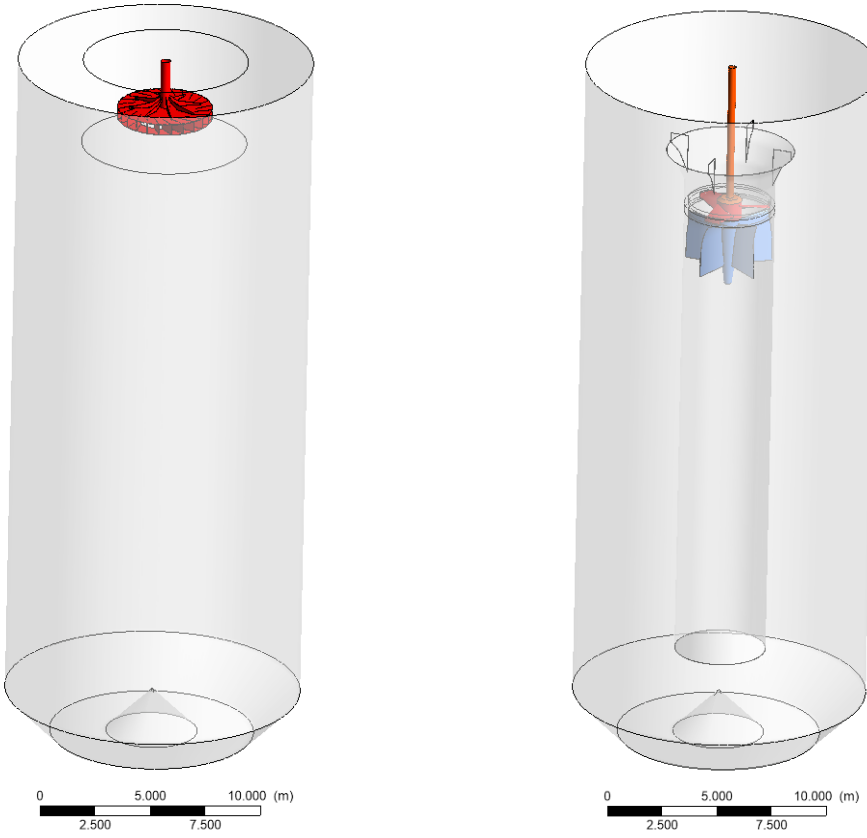

(a) (b)

Figure 4. Geometries generated using Ansys DesignModeler for the industrial application of: (a) Full-scale SWIRLFLOW® tank; (b) Full-scale draft tube tank.

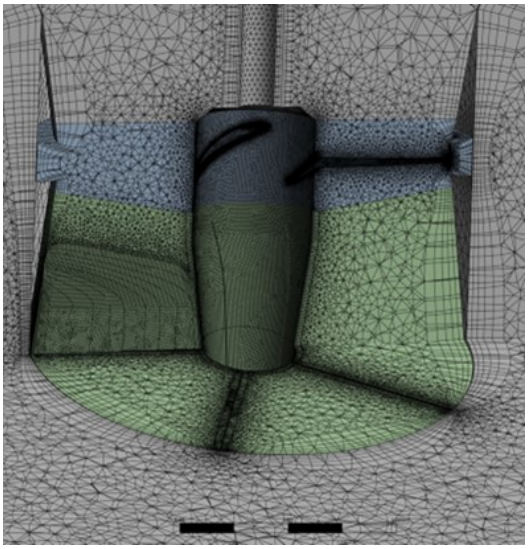

Figure 5. Close-up view of the mesh generated near the impeller region for the draft tube tank.

3. Results and Discussion

3.1 Lab-scale Analogue Tanks

3.1.1 Scale Formation Experiments

CSIRO has developed a laboratory methodology for studying scale formation using mixing tanks designed as geometric analogues of full-scale industrial precipitators. The detailed setup has been documented elsewhere [2, 3], and a brief summary is provided here to aid interpretation of CFD results. A gypsum scale system was created based on a neutralisation reaction between sulphuric acid and calcium carbonate. Laboratory tests were conducted in stainless steel tanks of 2 litre and 50 litre capacity, under controlled agitation conditions using conventional and SWIRLFLOW® impellers. Scale was grown over a multi-day period through sequential chemical dosing, and the resulting deposition was quantified using three-dimensional laser scanning and visual inspection. The observed scale morphology and distribution patterns closely matched those observed in full-scale operations, validating the effectiveness of the experimental approach. Figure 6 shows photographs of the scale pattern observed after liquid removal in the 2 L tank (Figure 6a) and 50 L tank (Figure 6b). Figure 6c presents a laser-scanned contour map of the 50 L tank. These results provided a robust basis for assessing validity of the CFD models and for correlating predicted wall shear stress with actual scale accumulation under various agitation regimes.

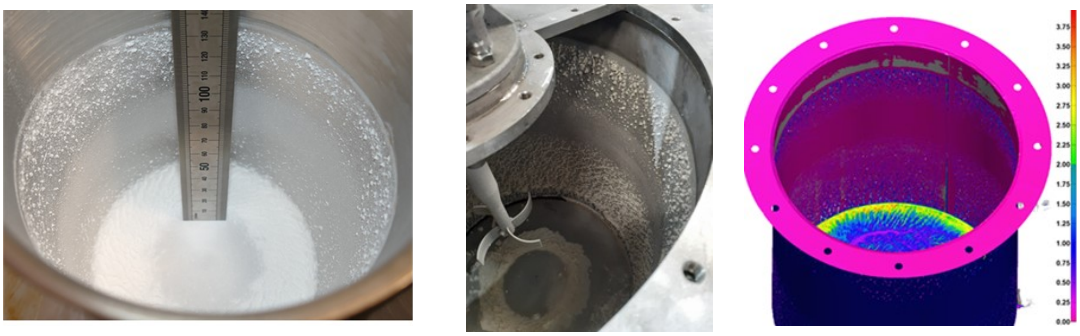

(a) (b) (c)

Figure 6. Experimental results: (a) scale formation photograph in 2 L tank; (b) scale formation photograph in 50 L tank; (c) laser scan of scale distribution in 50 L tank.

3.1.2 Flow Patterns

Figure 7 uses three-dimensional streamlines to illustrate the flow structures in the 2 L and 50 L SWIRLFLOW® tank cases. For simplicity and representativeness, only results for one impeller speed are shown for each tank. The rotating impeller drives fluid radially outward, creating a low-pressure zone that draws liquid from above and below into the impeller region. The outward jet impinges on the tank wall and splits into upward and downward streams, forming two local recirculation loops. At the same time, the rotation of the impeller induces strong horizontal swirling motion throughout the tank. The vertical position of the impeller influences the asymmetry of the flow, with stronger recirculation either above or below the impeller depending on its clearance from the tank bottom. Despite the difference in scale, the 2 L and 50 L tanks demonstrate similar overall flow characteristics.

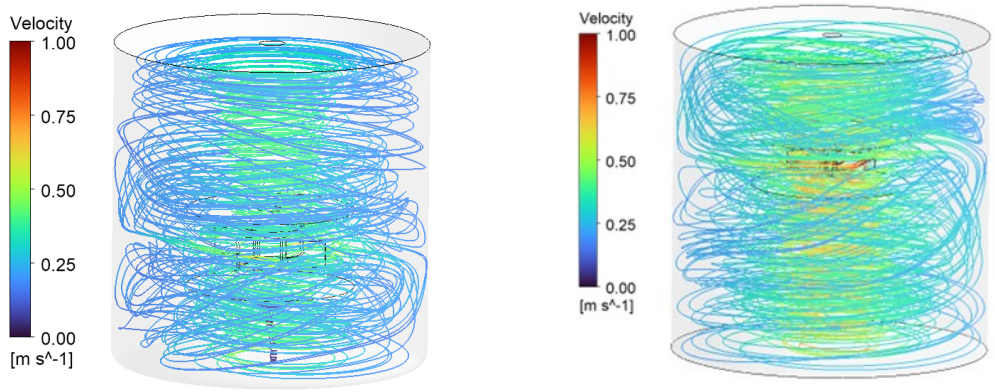

(a) **(b)**

Figure 7. Flow characteristics visualised by 3D streamlines for (a) 2 L tank at 300 rpm and (b) 50 L tank at 250 rpm.

Figure 8 presents the wall shear stress distribution on the walls of the same tanks. Consistent with the flow structures, elevated wall shear stress is observed near the impeller region. The highest shear occurs at the centre of the tank bottom, where the downward flow along the walls and across the tank base converges and transitions into an upward flow along the central axis. This high-shear region corresponds to areas with minimal scale deposition observed in experiments, as shown in Figure 6. In contrast, regions of lower wall shear stress – particularly near the upper tank walls and outer edges – correlate with heavier scale accumulation.

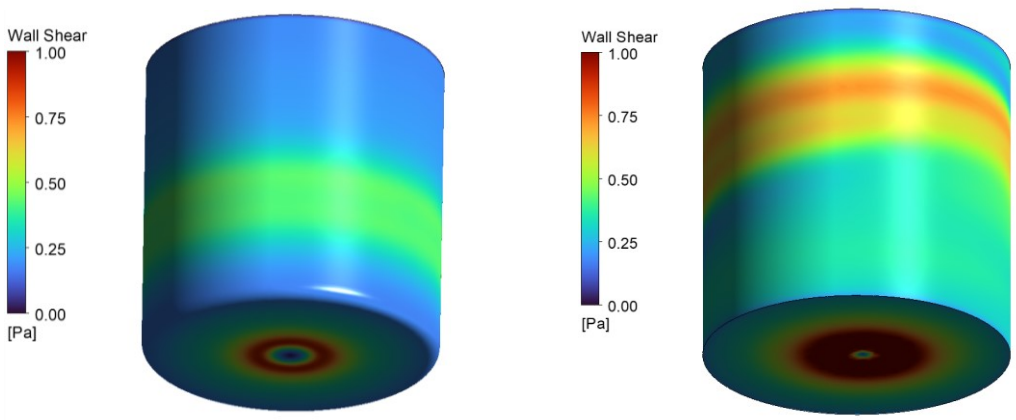

(a) **(b)**

Figure 8. Wall shear stress from CFD for (a) 2 L tank at 300 rpm and (b) 50 L tank at 250 rpm.

The qualitative correlation between flow-induced wall shear stress and scale distribution provides justification for a more detailed quantitative comparison. This relationship – linking measured scale thickness with CFD-predicted wall shear stress – is further examined in the following section.

3.1.3 Correlation between Scale Formation and Wall Shear Stress

For the 2 L tank experiment, the scale deposits were carefully scraped off the tank walls and collected to determine the total scale mass. Figure 9a illustrates the total scale mass measured, revealing an exponential decrease in scale accumulation with increasing impeller speed. To investigate the relationship between scale formation and wall shear stress, the average wall shear stress on the tank walls was computed using CFD simulations. Based on the assumption that higher wall shear stress is associated with reduced scale deposition, the wall shear stress data is presented in a reciprocal format. This approach demonstrates a strong alignment between the trend observed in Figure 9a and that depicted in Figure 9b, underscoring the inverse correlation between wall shear stress and scale formation.

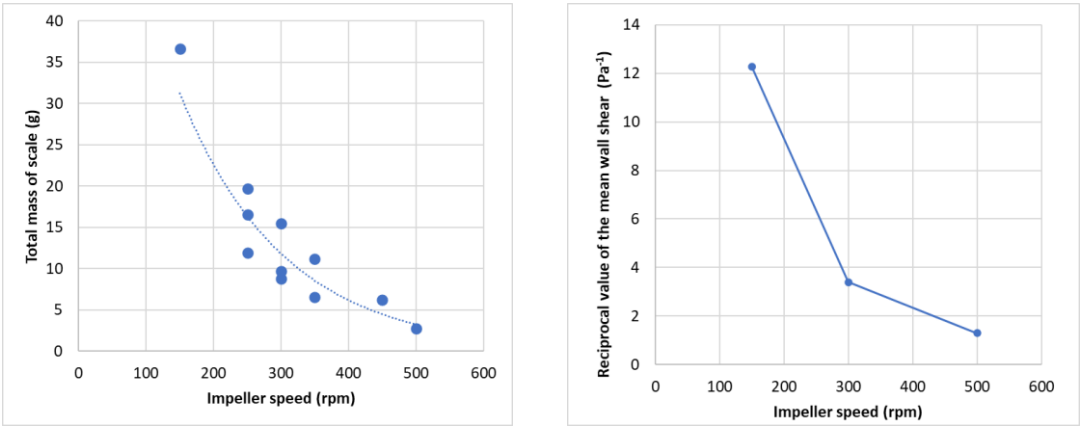

(a) **(b)**

Figure 9. Impact of impeller speed in 2 L Tank: (a) Total mass of scale (Experiment); (b) Reciprocal value of the averaged tank wall shear (CFD).

From Figure 6a, it can be seen that two distinct regions of scale deposition are present at the bottom of the 2 L tank. A central region exhibits only a thin layer of scale, surrounded by an outer region where the scale thickness increases progressively toward the tank wall. This central, low-scale region is a result of the swirling flow creating elevated wall shear stress near the centre. As the impeller speed increases, the diameter of this reduced-scale region also increases, indicating stronger swirl-induced shear.

Figure 10a shows the measured diameter of the central reduced-scale zone as a function of impeller speed, based on manual measurements using dividers and a steel ruler. The diameter of this low-scale region increases almost linearly with increasing rotation speed, indicating enhanced wall shear from the swirl flow. As shown in Figure 7, the flow pattern near the bottom wall involves downward motion along the tank periphery, which converges near the base and rises upward at the centre. This results in maximum wall shear stress at the centre and minimum near the edges – closely aligning with the observed scale patterns.

The outer edge of the reduced-scale zone, as identified from experimental observations, may correspond to a specific wall shear stress level – interpreted as the critical shear threshold for scale inhibition. This threshold, estimated from CFD results, is plotted against impeller speed in Figure 10b. Notably, the critical value is not fixed; rather, it increases almost linearly with rotation

speed. This trend suggests that wall shear stress is not the sole factor required to suppress scale formation and that it might depends on other factors such as the local flow regime, residence time, chemical composition and/or energy input. Further investigation is warranted to better understand the underlying physical mechanisms governing this relationship.

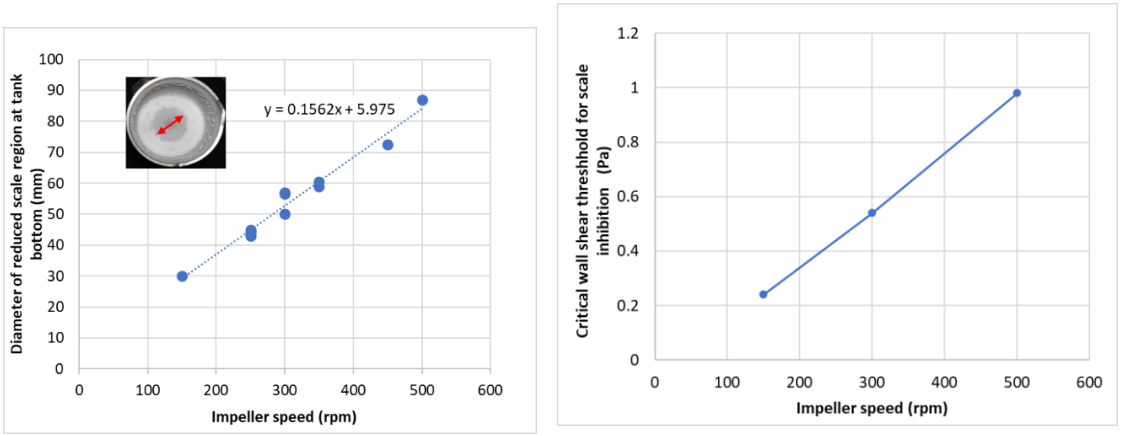

(a) **(b)**

Figure 10. Impact of impeller speed in 2 L tank: (a) Measured diameter of the reduced-scale zone; (b) Critical wall shear stress at the boundary of the reduced-scale zone.

For the 50 L tank experiment, laser scanning was performed across the tank side wall, allowing for quantification of scale thickness at different heights. Figure 11a presents the scale thickness measured via laser scanning, revealing that increasing impeller speed correlates with notably reduced scale formation, particularly evident near the impeller. To investigate the relationship between scale formation and wall shear stress, Figure 11b depicts the CFD calculated wall shear stress distribution in reciprocal format as a function of height and impeller speed. The variation in wall shear stress shows some similarity to the observed scale patterns in Figure 11a, showcasing reduced scale formation at higher wall shear stress levels. While employing a reciprocal format for wall shear values may offer a different perspective, it is important to recognize that scale formation is influenced by multiple interacting factors, including the local flow regime, residence time, chemical composition, and energy input. These factors collectively determine the thickness and structure of the deposited scale.

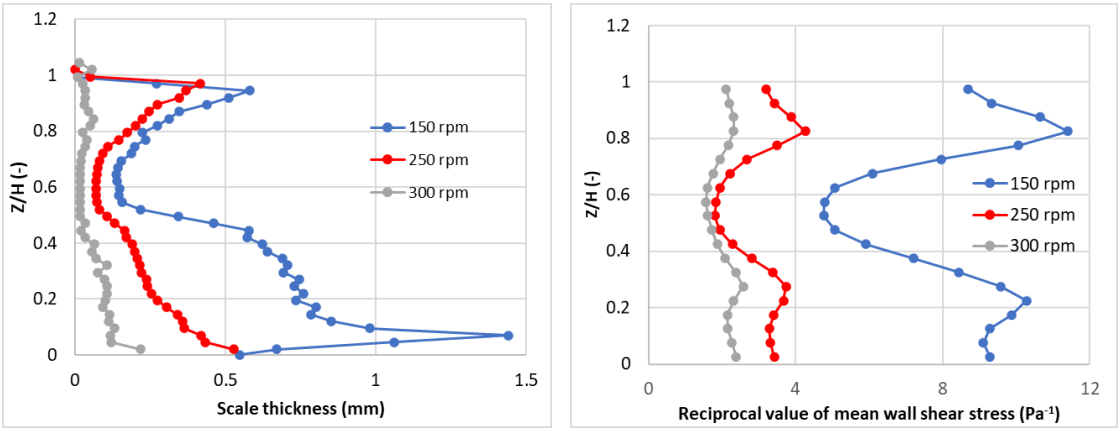

(a) **(b)**

Figure 11. 50 L tank: (a) Measured mean scale height as a function of impeller speed; (b) Variation of side wall shear stress with height at different impeller speeds from CFD simulations.

3.2 Industrial-Scale Draft Tube Tanks vs. Swirl Flow Tanks

The correlation inferred in the previous section between experimental scale measurements and CFD-predicted wall shear stress in the lab-scale tank suggests the potential of CFD modelling as a tool for understanding scale formation. This validation provides a strong foundation for extending CFD analysis to industrial-scale systems, particularly given the cost and logistical challenges of conducting experiments at full scale. In this section, CFD is used to compare the performance of draft tube and SWIRLFLOW® configurations in full-scale precipitator tanks. This analysis highlights key differences in flow patterns and their potential implications for scale mitigation.

3.2.1 Flow Patterns

Figure 12 shows flow characteristics visualised by 3D streamlines for the draft tube tank (Figure 12Figure 12a) and the SWIRLFLOW® tank (Figure 12b). In the draft tube configuration, liquid is drawn downward through the impeller located inside the draft tube. Upon exiting the draft tube at its bottom, the flow impinges on the tank base and is redirected upward along the annular region outside the tube, forming a primary circulation loop. This upward flow eventually re-enters the top of the draft tube, establishing a global recirculation pattern. In addition to this primary recirculation, several strong local recirculation zones are observed in the lower half of the tank, outside the draft tube. These ones suggest that a fair portion of the liquid does not fully engage in the global flow pattern. For the SWIRLFLOW® tank, the flow pattern resembles those observed in the 2 L and 50 L tanks discussed earlier and is therefore not described in detail here.

Figure 13 presents the velocity vector distribution on a vertical plane. The SWIRLFLOW® configuration exhibits a strong upward velocity at the tank centre, which is favourable for solids suspension and scale mitigation. The CFD results also reveal significant swirling motion with a strong horizontal velocity component near the wall, promoting more uniform flow distribution compared to the draft tube configuration. In contrast, the draft tube tank displays a predominantly vertical flow pattern, characterised by downward flow through the draft tube and upward flow in the outer region, with limited horizontal mixing. The enhanced swirl and wall shear in the SWIRLFLOW® design are key features contributing to reduced scale formation.

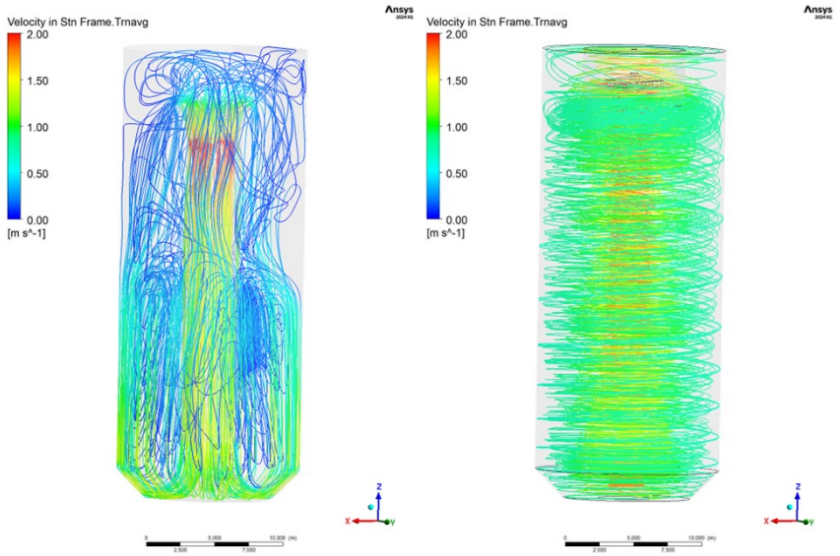

(a) (b)

Figure 12. Flow characteristics visualized by 3D streamlines for (a) the draft tube tank and (b) the SWIRLFLOW® tank.

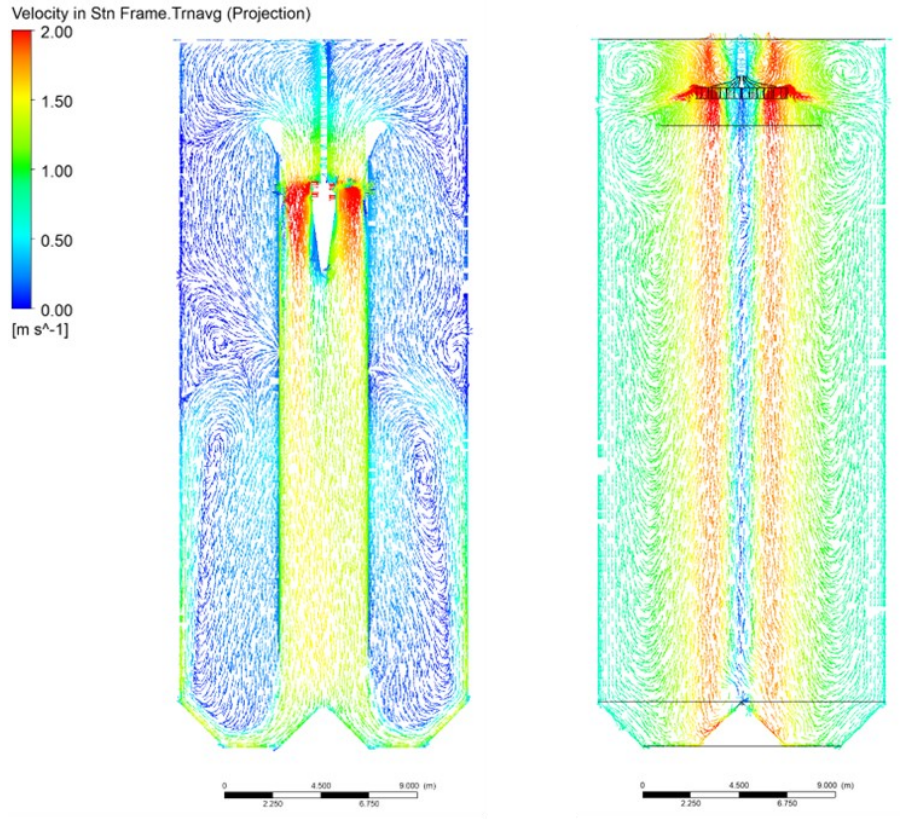

(a) (b)

Figure 13. Velocity vector distribution along a vertical plane across the tank axis for (a) the draft tube tank and (b) the SWIRLFLOW® tank.

3.2.2 Wall Shear Stress

Given the good inverse correlation between wall shear stress and scale formation, it is valuable to further examine the wall shear stress distribution in the full-scale tanks. Figure 14 presents wall shear stress profiles on the tank side walls, which are consistent with the flow structures discussed in the previous section. In the draft tube tank, two distinct regions are observed: high wall shear stress near the bottom and very low shear in the upper section (Figure 14a). In contrast, the SWIRLFLOW® tank shows a more uniform distribution, with elevated shear concentrated around the impeller region (Figure 14d).

Figure 14 (b) and (c) show the wall shear stress on the outer and inner surfaces of the draft tube, respectively. The inner surface exhibits substantially higher shear stress than the outer surface. These results are consistent with laboratory findings from draft tube scale tests (Figure 15) and plant observations, which confirm that regions of low wall shear—particularly the outer draft tube surface and the upper tank walls—are prone to heavy scale accumulation, while the high-shear inner surface remains largely free of scale. In some cases, scale thickness on the draft tube tank wall can exceed 500 mm, and the associated weight can lead to structural failures, such as draft tube collapse. Scale in draft tube tanks versus SWIRLFLOW® tanks is further discussed in Wu et al (2021) [4] based on plant experience.

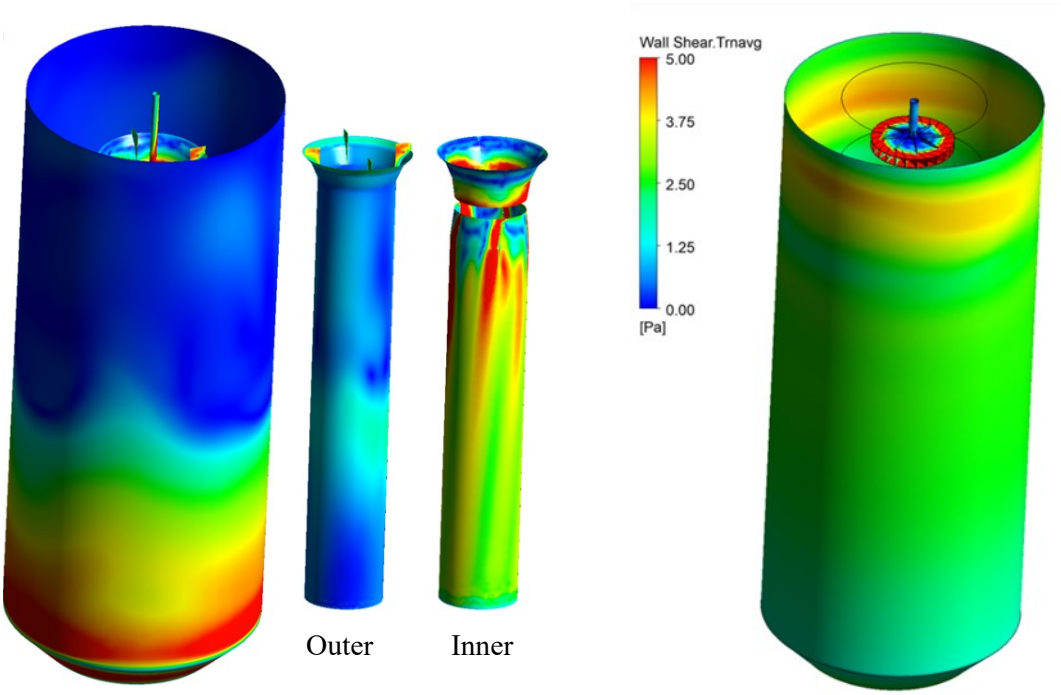

Figure 14. Wall shear stress distribution along the side walls of: (a) the outer tank wall of the draft tube tank; (b) the outer surface of the draft tube; (c) the inner surface of the draft tube; (d) the SWIRLFLOW® tank.

Figure 15. Visualization of scale formation on a laboratory draft tube tank.

3.2.3 Effect of Tank Type on Agglomeration

The calculation of flow fields in precipitators via CFD allows access to fundamental properties of turbulent flows which can provide useful information about the precipitator's performance. The example discussed in the present work is the effect of precipitator agitation strategy on agglomeration and the risk of particle collisions which can disrupt agglomerations.

Following Rijkboer et al (2022)[5], the parameters of interest are the Taylor microscale and the Kolmogorov microscale.

Both of these parameters can be calculated from the output of turbulent CFD calculations using the following equations:

$$\lambda_k = \left(\frac{\nu^3}{\varepsilon}\right)^{1/4} \quad (1)$$

$$\lambda_g = \theta \left(\frac{60\nu}{\varepsilon}\right)^{1/2} \quad (2)$$

where:

λ_k Kolmogorov microscale of turbulence, m
λ_g I Taylor microscale of turbulence, m
ν Kinematic viscosity, m^2/s
ε energy dissipation rate per unit mass, J/s·kg
θ fluctuating average component of local velocity, m/s

It was of interest to compare these values from draft tube to SWIRLFLOW® precipitators to evaluate if there were any significant differences which could indicate a changed particle collision regime. In particular, the primary interest was if there was a difference in particular attrition between the agitation types. Figure 16 shows a comparison of the Taylor microscale between the Draft Tube and SWIRLFLOW® cases. It is seen that for most of the tanks' volume, the Taylor microscale exceeds 0.015 m apart from the vicinity of the impellers. Similarly, the results for the Kolmogorov microscale are shown in Figure 17.

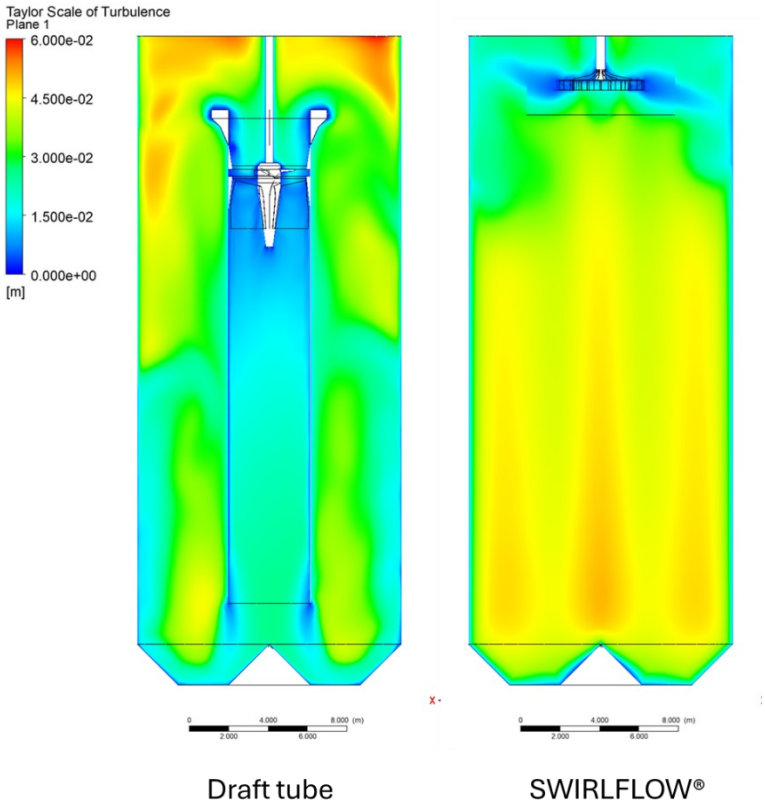

Figure 16. Comparison between Draft Tube and SWIRLFLOW® for the Taylor microscale.

Again, the microscale exceeds 125 microns throughout most of the tank for both types of agitation. These results suggest that given the bulk of alumina hydrate particles are smaller than the turbulence microscales present throughout most of the tank's volume, the particles would likely not suffer from turbulence induced collisions or attrition. In any case, the difference between the two types of tank agitation, in terms of particle collisions should be small given that in both cases, the microscales are mostly larger than typical particles.

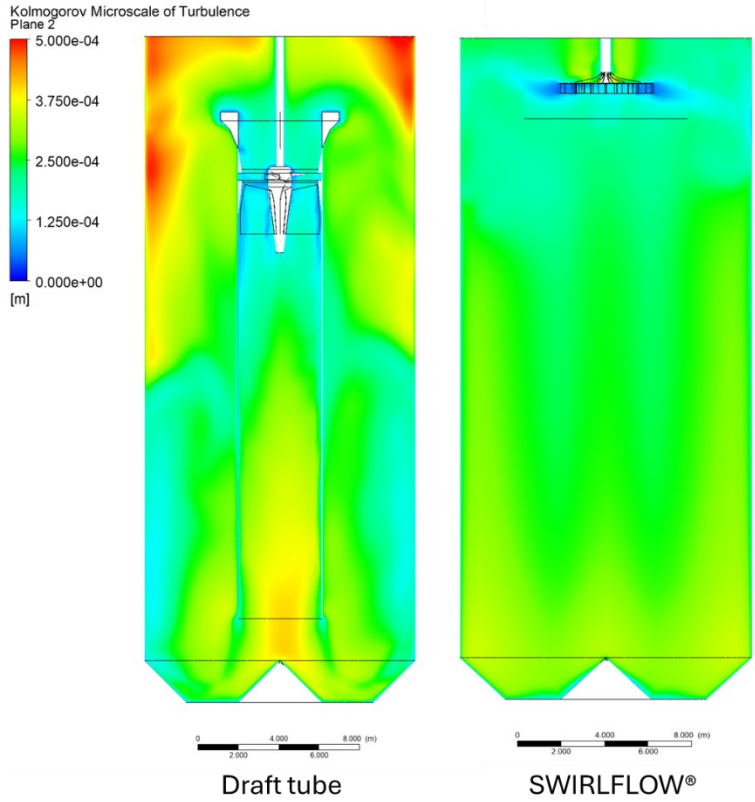

Figure 17. Comparison between Draft Tube and SWIRLFLOW® for the Kolmogorov microscale.

4. Conclusions

A CFD model was developed to investigate flow characteristics and wall shear stress in laboratory and industrial-scale precipitator tanks. For the laboratory-scale SWIRLFLOW® tanks, wall shear stress predicted by CFD was related with experimentally measured scale formation. The total scale mass was found to decrease with increasing wall shear stress, and the spatial distribution of low-shear regions corresponded well with areas of heavy scale accumulation.

For the industrial-scale tanks, CFD simulations compared the flow behaviour of a draft tube tank and a SWIRLFLOW® tank. The severe scale formation observed in draft tube configurations was well explained by the presence of low-shear regions on the outer draft tube wall and upper tank surfaces. In contrast, the SWIRLFLOW® tank exhibited a more uniform shear stress distribution with elevated values near the impeller, effectively reducing scale formation.
These CFD simulations, validated by experimental observations, provide new insight into the mechanisms of scale control and offer a predictive framework for the evaluation and optimisation of agitation systems in industrial precipitation tanks.

Further extraction of turbulent microscales from the CFD simulations have shown that microscales associated with turbulence are larger than typical hydrate particles over most of the tank volume for both Draft Tube and SWIRLFLOW® agitation. This result suggests that the particle attrition behaviour is likely similar between the two agitation types.

5. References

1. Julie Townsend et al., Reflections on 25 years of SWIRLFLOW® operation at QAL alumina refinery, *Proceedings of 42nd International ICSOBA Conference,* Lyon, France, 27 – 31 October 2024, *TRAVAUX* 53, 481-483. https://doi.org/10.71659/icsoba2024-aa021
2. Jie Wu et al., An analogous scale model for laboratory mixing studies, *Mineral Enginnering*, Vol 199, (2023) 1081111. https://doi.org/10.1016/j.mineng.2023.108111
3 Shen, L. et al., The effect of impeller speed on scale formation within a swirling flow tank, *24th Australasian Fluid Mechanics Conference (AFMC 2024)*, 1-5 December 2024, Canberra. Australia.
4 Jie Wu et al., Increased agitation reliability for slurry suspension in mineral processing, *Minerals Engineering,* Vol. 170, 2021, 107008. https://doi.org/10.1016/j.mineng.2021.107008
5. Rijkeboer, Ab, McFeaters, J. and Manché, D, Advances in process simulation of agglomeration in Bayer precipitation, *Proceedings of 40th International ICSOBA Conference,* Athens, Greece, 10 – 14 October 2022, *TRAVAUX* 51, 397-414.